Chemical Science

ROYAL SOCIETY OF CHEMISTRY

EDGE ARTICLE

View Article Online
View Journal | View Issue

Cite this: *Chem. Sci.*, 2025, **16**, 17316

All publication charges for this article have been paid for by the Royal Society of Chemistry

Received 24th May 2025
Accepted 25th August 2025

DOI: 10.1039/d5sc03774c

rsc.li/chemical-science

Copper-catalysed oxy-alkylation of styrenes enabled by halogen-atom transfer

Qiujian Tan,†[ab] Xiang Lyu, †[c] Yu Zhao,[a] Huaquan Fang,*[b] Xianxiu Xu *[a] and Zhongyan Hu *[a]

Herein, we present a mechanistically distinct approach to the multicomponent difunctionalisation of styrenes with alkyl halides and oxygen by integrating α-aminoalkyl radical-mediated halogen-atom transfer (XAT) with copper catalysis under air-equilibrated conditions. This strategy eliminates the need for external peroxides or photoredox conditions, offering a streamlined and efficient alternative. Mechanism studies uncover a unique role for the copper catalyst: instead of directly activating alkyl halides, inexpensive $CuCl_2$ oxidizes a tertiary amine to generate an α-aminoalkyl radical, which then drives XAT to release alkyl radicals. These radicals subsequently add to alkenes, facilitating efficient difunctionalisation. This method accommodates a broad range of alkyl radical precursors, including fluoroalkyl- and alkyl halides, and demonstrates compatibility with diverse styrenes, enabling the modular synthesis of β-(fluoro)alkylated ketones with excellent functional group tolerance under mild conditions. Notably, the strategy's practical utility is exemplified through the late-stage functionalisation of biologically active molecules and pharmaceuticals, showcasing its potential for rapid, efficient access to structurally complex molecules.

Introduction

The accessibility and versatile reactivity of carbon–carbon double bonds make alkenes a sought-after class of feedstocks in chemical synthesis.[1] Over the past few decades, numerous efficient strategies have been developed for their functionalisation.[2] Among these, the catalytic difunctionalisation of styrenes has emerged as a particularly powerful approach for enhancing molecular complexity by simultaneously installing two distinct functional groups across the double bond in a single transformation.[3] Alkyl halides, due to their structural diversity and synthetic accessibility, have become some of the most widely employed reagents in organic chemistry, serving as excellent precursors for generating alkyl radicals.[4] In this context, the catalytic alkylation of styrenes with alkyl halides has become a vibrant area of research in both transition metal and photoredox catalysis (Scheme 1a). These approaches typically rely on direct single-electron transfer (SET) between metal (*e.g.*, Ni,[5,6] Co,[7,8] Pd,[9,10] Cu,[11–13] and Fe[14]) or photoredox catalyst[15,16] and the alkyl halides to generate the corresponding alkyl radicals.[5–16] However, their general applicability is often constrained by substrate-specific reactivity, with optimal performance typically observed for activated halides such as ethyl bromodifluoroacetate. In contrast, unactivated alkyl halides present a substantial challenge due to their intrinsically more negative reduction potentials (<−2 V *vs.* SCE),[17–20] necessitating strongly reducing conditions that are often incompatible with mild radical initiation. Seminal work by the groups of

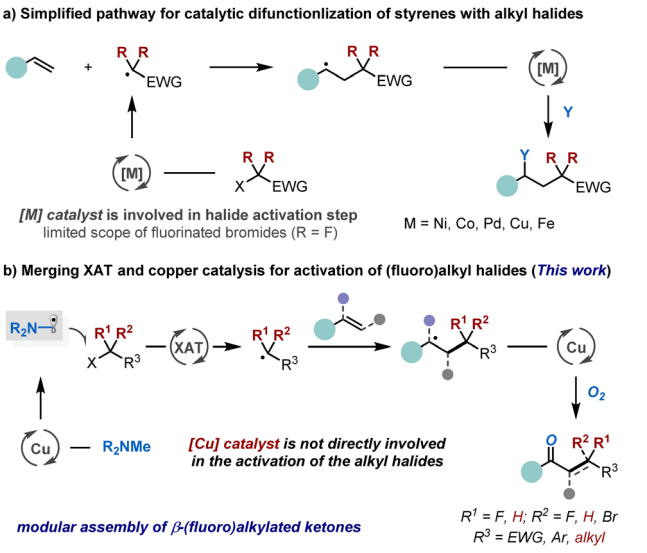

Scheme 1 Radical-mediated difunctionalisation of styrenes with alkyl halides.

[a]College of Chemistry, Chemical Engineering and Materials Science, Shandong Normal University, Jinan 250014, China. E-mail: xuxx677@sdnu.edu.cn; huzy@sdnu.edu.cn
[b]School of Pharmaceutical Sciences, Chongqing University, Chongqing 401331, China. E-mail: fanghq@cqu.edu.cn
[c]School of Pharmaceutical Sciences, Institute of Materia Medica, Shandong First Medical University, Jinan 250117, China
† These authors contributed equally.

Huang,[5,8] Lei,[7] Zhang,[6] and others[5–16] has demonstrated that cobalt-, nickel-, or palladium-catalysed processes, employing electron-shuttle catalysis,[5,8] halogen-atom transfer (XAT),[7] photoinduced systems,[10] or organolithium reagents as coupling partners,[6] can promote electron transfer from low-valent metal species to alkyl halides, thereby facilitating alkene functionalisation. While these advances represent significant progress, the pursuit of a low-cost and green alternative strategy for styrene alkylation, capable of enabling simpler, milder, and more efficient activation of alkyl halides with broad functional group compatibility, remains a crucial and highly sought-after objective.[21–23]

Recent studies have revealed that alkyl radicals can be efficiently generated from their corresponding halides by leveraging α-aminoalkyl radicals to trigger XAT reactions.[18–20,24–26] This strategic approach leverages strong polar effects in the transition state during halide abstraction, thereby facilitating alkyl radical formation.[18–20,24–30] As a result, the alkyl halide is not required to engage in direct SET with the metal,[19] nor coordination with it for subsequent abstraction or oxidative addition,[13,31,32] thereby enabling broader synthetic applications. Building on these insights, we hypothesized a conceptually distinct strategy where the copper catalyst facilitates the formation of α-aminoalkyl radical without directly activating the alkyl halide.[33–37] This approach could offer significant synthetic advantages in assembling challenging small-molecule building blocks. The proposed catalytic mechanism, illustrated in Scheme 1b, involves the copper catalyst preferentially oxidizing tertiary amines to generate α-aminoalkyl radicals, which then mediate XAT from alkyl halides, forming the corresponding alkyl radicals. These radicals subsequently add to alkenes, generating a new C-centered radical. The resulting intermediate undergoes recombination with oxygen (O_2) in the presence of the copper catalyst,[38] ultimately yielding the desired difunctionalisation product. The copper catalyst is continuously regenerated through electron exchange with the tertiary amine in the presence of O_2 from air. A key mechanistic distinction of this approach, compared to traditional transition-metal and photocatalysis systems, is that carbon–halogen bond activation occurs outside the copper catalytic cycle, independent of the nature of the copper catalyst and alkyl halide. This unique feature also eliminates the need for expensive catalysts and additional photocatalysis,[39,40] which we anticipate will broaden the substrate scope and enhance the versatility of this transformation.

Results and discussion

Reaction development

To optimize the reaction conditions, a model reaction between styrene (**1**) and ethyl bromodifluoroacetate (**2**) was performed under air-equilibrated conditions (Table 1). After extensive screening (see the SI for details), we were pleased to find that ethyl (*Z*)-2-fluoro-4-oxo-4-phenylbut-2-enoate (**3**) was obtained in 73% yield with excellent regioselectivity ($Z/E > 22:1$) when $CuCl_2$ was used as the catalyst and *N*-cyclohexyl-*N*-methylcyclohexanamine (Cy_2NMe) was employed as the XAT reagent in MeCN at 25 °C

Table 1 Optimisation studies[a]

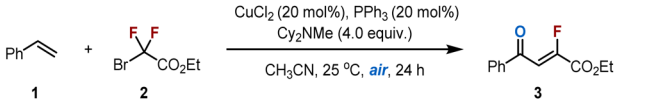

Entry	Variation from standard conditions	Yield of **3**[b] (%)	Z/E[b]
1	None	73 (71)[c]	>22 : 1
2	No $CuCl_2$	0	—
3	No Cy_2NMe	0	—
4	No PPh_3	62	>22 : 1
5	CuCl instead of $CuCl_2$	37	>22 : 1
6	$CuBr_2$ instead of $CuCl_2$	54	>22 : 1
7	$CoCl_2$/$PdCl_2$ instead of $CuCl_2$	0	—
8	Cy_2NEt instead of Cy_2NMe	17	>22 : 1
9	Pempidine instead of Cy_2NMe	47	>22 : 1
10	$^iPr_2NMe$ instead of Cy_2NMe	34	>22 : 1
11	Et_2NMe instead of Cy_2NMe	0	—
12	N_2 atmosphere	0	—
13	O_2 atmosphere	31	>22 : 1

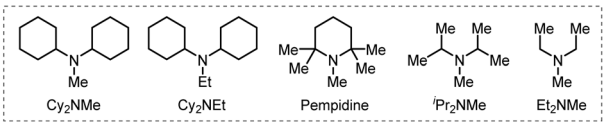

[a] Reaction conditions: **1** (0.3 mmol), **2** (1.2 mmol), $CuCl_2$ (0.06 mmol), PPh_3 (0.06 mmol), and Cy_2NMe (1.2 mmol) in CH_3CN (2 mL) at 25 °C under air atmosphere for 24 h. [b] Yields and Z/E ratios were determined by ^{19}F NMR analysis of the crude reaction mixtures using CF_3Ph as the internal standard. [c] Yield of isolated product.

(entry 1). Control experiments revealed that both $CuCl_2$ and Cy_2NMe were essential for the fluoroalkylation reaction (entries 2 and 3), and the absence of PPh_3 led to slightly decrease in yield (entry 4). Substituting $CuCl_2$ with other copper salts, such as CuCl or $CuBr_2$, resulted in lower yields, while other transition metals (*e.g.*, $CoCl_2$, $PdCl_2$) proved ineffective (entries 5–7). Notably, functionalized tertiary amines with less steric hindrance produced inferior results or failed entirely, underscoring the critical role of the sterically bulky Cy_2NMe (entries 8–11). Notably, air-equilibrated conditions are essential, no reaction occurs under a N_2 atmosphere (entry 12), while an O_2 atmosphere results in a decreased yield (entry 13). Finally, other difluoroalkyl radical precursors were examined. Chlorides proved unreactive, likely due to the stronger C–Cl bond.[17,41] Although more reactive, iodides afforded product **3** with reduced efficiency, likely due to the formation of Heck-type by-products, as evidenced by ^{19}F NMR analysis (Fig. S1).[42] We propose that, in the case of iodides, the newly radical formed *via* the initial addition step, undergoes rapid iodine atom transfer to generate an alkyl iodide, which subsequently undergoes dehydroiodination under the reaction conditions (Table S9).[43] These findings confirm that difluoroalkyl bromides deliver the best overall performance.

Oxo-fluoroalkylation of styrenes

With the optimized reaction conditions established, the substrate scope of the fluoroalkylation was initially explored

using fluorinated alkyl bromides (Scheme 2). This transformation demonstrated compatibility with a broad range of styrene-type olefins, including those with varying electronic properties at the *para*, *ortho*, or *meta* positions, affording the corresponding β-fluoroenone products **3–18** in moderate to good yields. Styrenes containing labile and synthetically versatile functional groups, including amines (**6**), halides (**8–10**, **18**), alcohols (**11**), silanes (**12**), boronic esters (**13**), alkenes (**14**), and alkynes (**15**),[44] were well-tolerated, offering opportunities for further derivatisation. Additionally, polysubstituted styrenes were also compatible, yielding the desired products (**19–20**) smoothly. Styrenes featuring fused arenes and heterocycles, such as naphthalene (**21**), thiophene (**22**), thiazole (**23**), benzofuran (**24**), benzothiophene (**25–26**), and carbazole (**27**) also proved compatible with this protocol, delivering the target products in moderate yields. Remarkably, radical precursors containing amides afforded the desired product **28**, while phosphonate groups resulted in the formation of β-fluoroenone **29** and an unexpected α-trifluoromethyl ketone **30** in moderate yields (Fig. S39).[45] Remarkably, 1,3-dienes, cyclic internal styrenes, and 1,2-diphenylethenes were all compatible with the reaction conditions, delivering the corresponding β-

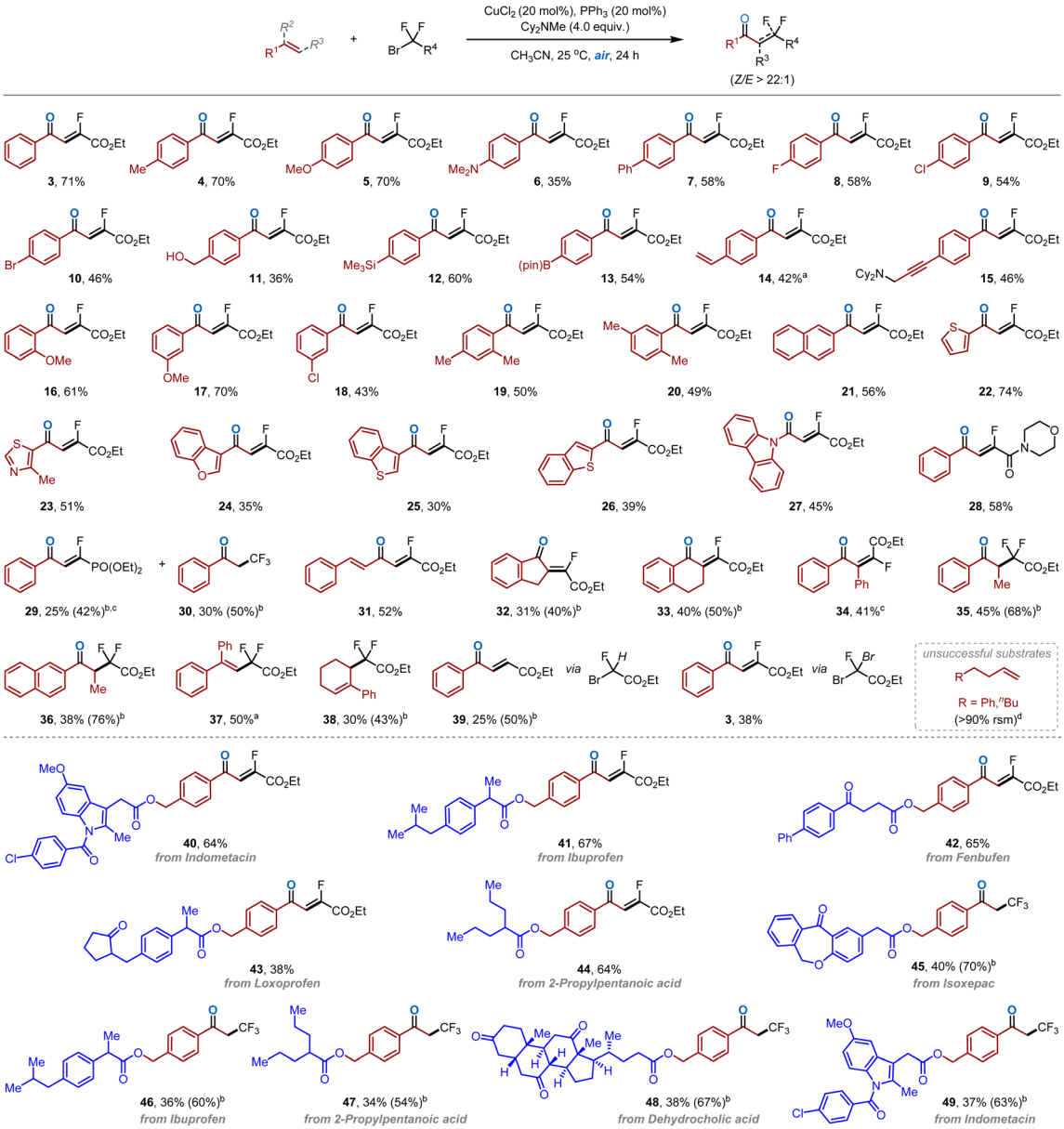

Scheme 2 Oxo-fluoroalkylation of styrenes with fluoroalkyl halides. Reaction conditions: styrenes (0.3 mmol), fluoroalkyl bromides (1.2 mmol), $CuCl_2$ (0.06 mmol), PPh_3 (0.06 mmol), and Cy_2NMe (1.2 mmol) in CH_3CN (2 mL) at 25 °C under air atmosphere for 24 h. [a]Styrenes (0.3 mmol), fluoroalkyl bromides (0.6 mmol), $CuCl_2$ (0.06 mmol), PPh_3 (0.06 mmol), and Cy_2NMe (0.6 mmol) in CH_3CN (2 mL) at 25 °C under air atmosphere for 24 h. Yield of isolated product, *Z*/*E* ratios were determined by ^{19}F NMR analysis of the crude reaction mixtures using CF_3Ph as the internal standard. [b]Yield based on recovered starting material. [c]*E*/*Z* > 22 : 1, the *E*-isomer is the major product. [d]No reaction, rsm = recovered of starting material.

fluoroenone products (**31–34**) in acceptable yields. The observed stereoselectivity of **34** can be rationalized by comparing the transition states energies leading to each isomer during the anti-fluoride elimination, as illustrated in Fig. S40. The transition state leading to (*E*)-**34** is energetically favored, as it avoids steric repulsion between the phenyl (Ph–) and alkoxycarbonyl (EtO_2C–) groups.[46] Interestingly, when (*E*)-β-methylstyrenes were empolyed under the standard condition, the non-defluorinated products (**35–36**) were obtained, likely due to steric hindrance that impedes the E2 elimination pathway.[47] Additionally, 1,1-disubstituted and 1,1,2-trisubstituted styrenes furnished the corresponding Heck-type products (**37–38**). This outcome is consistent with previous observations involving other catalytic systems utilizing α-aminoalkyl radical-mediated XAT strategies.[48] This method was also effective for mono-fluorinated substrates, as exemplified by the reaction of styrene with ethyl 2-bromo-2-fluoroacetate, which afforded the desired (*E*)-α,β-unsaturated ester **39**. Whereas ethyl di-bromofluoroacetate led to the formation of product **3** through debromination, rather than defluorination. However, unactivated olefins, such as 4-phenyl-1-butene and 1-octene, proved to be inefficient in this transformation, typically leading to the recovery of over 90% of the starting olefins (Fig. S17). Pyridine-containing olefins (*e.g.*, 4-vinylpyridine), which can act as ligands and interfere with the metal-catalytic system, also failed to undergo efficient transformation. Additionally, olefins with unique structural features, such as 1,3-enynes (*e.g.*, but-3-en-1-yn-1-ylbenzene) and allenes (*e.g.*, 1-phenylallene), led to complex reaction mixtures, complicating purification efforts. Biologically relevant olefins, derived from compounds such as indomethacin, ibuprofen, fenbufen, loxoprofen, and 2-propylpentanoic acid, were smoothly converted into β-fluoroenones **40–44** in moderate yields. Similarly, α-trifluoromethyl ketone derivatives **45–49** performed well under standard conditions, highlighting the potential utility of this method for late-stage diversification of pharmaceutical agents.

Synthetic transformations

To demonstrate the scalability of this fluoroalkylation, the reaction between **1** and **2** was scaled up to 1 mmol, yielding the desired product **3** in moderate yield (Scheme 3). While β-fluoroenones are intrinsically valuable,[49] their potential as synthetic intermediates were further showcased by converting **3** into versatile enaminones (**50–56**)[50] in high yields with excellent *E*-selectivity *via* a transition metal-free defluorination/amination or ammonolysis sequence.

Oxo-alkylation of styrenes

Building on the initial success, we next investigated the scope of the reaction with respect to unfluorinated alkyl halides (Scheme 4). We were pleased to observe that a broad range of alkyl bromides successfully participate in the reaction with various styrenes, leading to the formation of a diverse array of γ-ketoesters (**57–68**) in moderate to good yields. Notably, γ-ketoester **57** could be obtained on a large-scale with a 60% isolated yield. Furthermore, α-bromo amides were also compatible with the

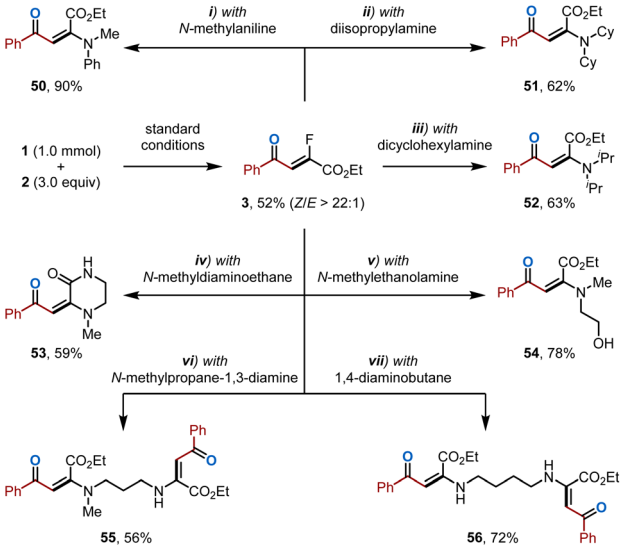

Scheme 3 Scale-up reaction and synthetic transformations.

reaction, providing the desired products **69–70**, which feature both oxo and amino groups, making them valuable for subsequent transformation. Additionally, a variety of α-bromoketones was incorporated into the method, yielding structurally diverse 1,4-dicarbonyl compounds (**71–74**). These compounds present a synthetic challenge due to the intrinsic polarity mismatch of the substrates,[51] demonstrating the broad applicability of the protocol. α-Bromonitrile was also a suitable partner, delivering the synthetically valuable β-nitrile ketone **75** in moderate yield. Ethyl dibromoacetate also participated in this transformation, resulting in the formation of the debromination product **39**. Notably, unactivated alkyl halides, such as benzyl bromides (*e.g.*, (bromomethyl)benzene) and alkyl iodides (*e.g.*, 1-fluoro-2-iodoethane, 1-iodo-3,3,3-trifluoropropane, and 1-iodo-4,4,4-trifluorobutane), were successfully incorporated into this platform, affording the desired products **76–79**. However, most of other alkyl bromides proved inefficient in this transformation, with the aminomethylation[28] or E2 elimination[30] by-products detected by high-resolution mass spectrometry (HRMS) analysis (Fig. S18–S29). Attempts to improve reactivity by using more electrophilic Michael acceptors (*e.g.*, ethyl acrylate, acrylonitrile, 1-phenylprop-2-en-1-one, and cinnamonitrile) were also unsuccessful under the current conditions (Fig. S30–S33). We speculate that in these cases, α-aminoalkyl radical-mediated XAT is slowed due to the stronger nature of the C–Br bond,[41] making the direct Giese addition of alkyl radicals to the acceptor more competitive.[18,43] This reactivity gap is especially pronounced under aerobic conditions.[52] Finally, this protocol was shown to be effective in late-stage modification of complex molecules, as exemplified by compounds **80–86**, where biorelevant groups were incorporated to afford the desired 1,4-dicarbonyl products in moderate to high yields.

Mechanistic investigations

To gain insight into the reaction mechanism, a series of control experiments were conducted. First, radical trapping

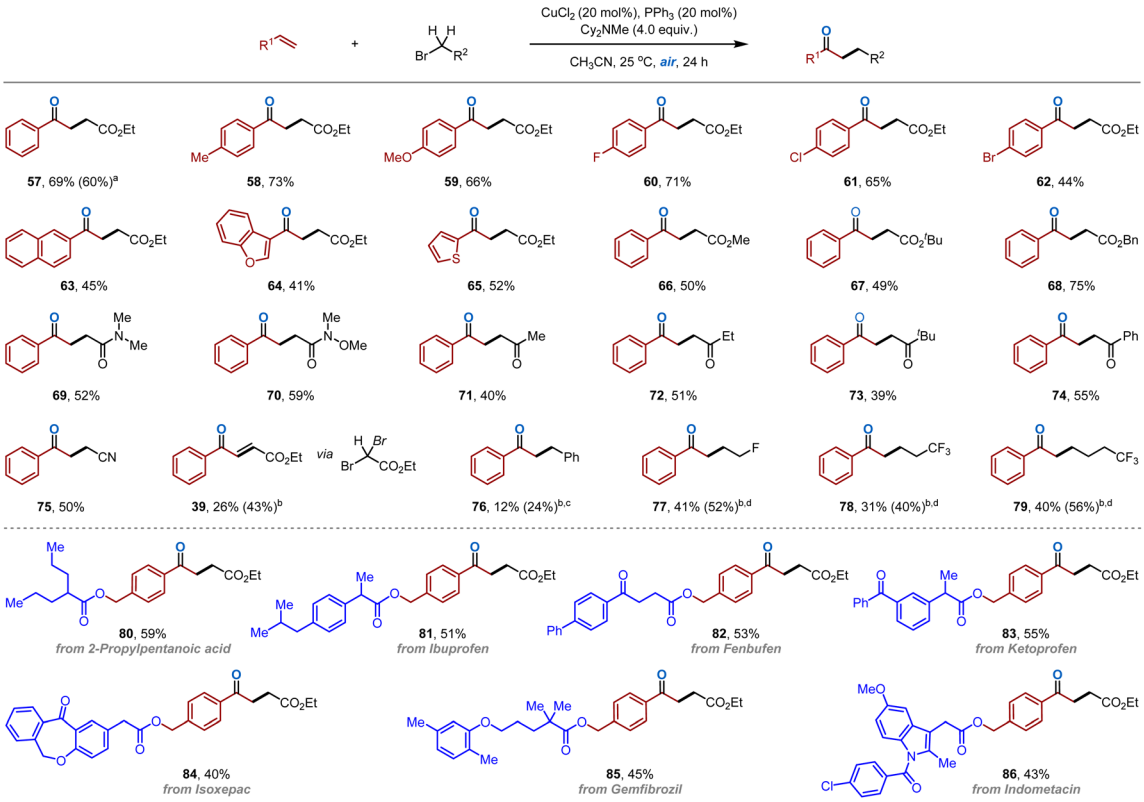

Scheme 4 Oxo-alkylation of styrenes with alkyl halides. Reaction conditions: styrenes (0.3 mmol), alkyl halides (1.2 mmol), $CuCl_2$ (0.06 mmol), PPh_3 (0.06 mmol), and Cy_2NMe (1.2 mmol) in CH_3CN (2 mL) at 25 °C under air atmosphere for 24 h. [a]1.0 mmol scale experiment, alkenes (1.0 mmol), alkyl halides (2.0 mmol), $CuCl_2$ (0.06 mmol), PPh_3 (0.06 mmol), and Cy_2NMe (2.0 mmol) in CH_3CN (4 mL) at 25 °C under air atmosphere for 24 h. Yield of isolated product. [b]Yield based on recovered starting material. [c]20% benzaldehyde isolated as a by-product. [d]Alkyl iodides were used.

experiments were performed using 2,2,6,6-tetramethylpiperidinyl-1-oxide (TEMPO) and 2,6-di-*tert*-butyl-4-methylphenol (BHT) as radical scavengers each separately (Scheme 5a). The reaction was completely inhibited in the presence of TEMPO, while the formation of product **3** was significantly reduced in the presence of BHT. In addition, several radical-adducts were observed and characterized, including difluoroalkyl-TEMPO (**S1**), α-aminoalkyl-TEMPO (**S2**), difluoroalkyl-BHT (**S4**), and α-aminoalkyl-BHT (**S5**), through ^{19}F NMR and HRMS analysis (Fig. S2 and S3).[6,53] These findings suggest that the reaction likely proceeds *via* a radical pathway. Further radical trapping studies using 1,1-diphenylethylene revealed the presence of a C-centered radical species (**S6**) and oxo-difluoroalkylation products (**3′**), with the difluoroacetate adduct **37** isolated in 34% yield (Scheme 5b and Fig. S4).[54] Additionally, the detection of iminium ion **S3**, ammonium salts **S7** and **S8** suggests that Cy_2NMe is involved in both the XAT and defluorination steps. To further confirm the involvement of a difluoroalkyl radical in the reaction, a radical-clock experiment was conducted. As shown in Scheme 5c, treatment of compound **87**, known to undergo radical rearrangement, with **1** and **2** under standard conditions afforded the ring-expanded product **88** in 40% yield (determined by ^{19}F NMR spectroscopy), along with 33% yield of **3** (Fig. S5).[55–57] These results support the involvement of an ethyl difluoroacetate radical and confirm that the reaction proceeds *via* a radical-mediated Giese-type mechanism.[58] Consistent with this mechanistic hypothesis, intermediate **3′** was detected by ^{19}F NMR and HRMS upon lowering Cy_2NMe and shortening the reaction time (Fig. S6), supporting its conversion to β-fluoroenones **3** *via* dehydrofluorination.[59]

To further investigate the conversion of fluoroalkyl halides and amines, electron paramagnetic resonance (EPR) experiments were conducted using phenyl *N*-*tert*-butylnitrone (PBN). In the reaction of **1** with **2** under standard conditions, the formation of the PBN-spin adduct **R1** indicates the selective generation of the ethyl difluoroacetate radical (Scheme 5d).[6,54,60] When **2** was reacted alone, a new PBN-spin adduct (**R2**) was observed, which was assigned as the α-aminoalkyl radical based on its spectral characteristics,[61,62] confirmed through HRMS analysis (Fig. S7 and S8). Furthermore, in the presence of both $CuCl_2$ and Cy_2NMe, the PBN-spin adduct **R3**, generated from the reaction of amine radical cation with PBN, was entrapped (Scheme 5e and Fig. S9).[63,64] In contrast, no radical species were observed when $CuCl_2$ was replaced by CuCl under the same conditions (Fig. S10). Notably, when a mixture of $CuCl_2$, **2**, and PBN was used, no difluoroacetate radicals were observed in the EPR spectrum, and a band with *g*-values around 2.134 was

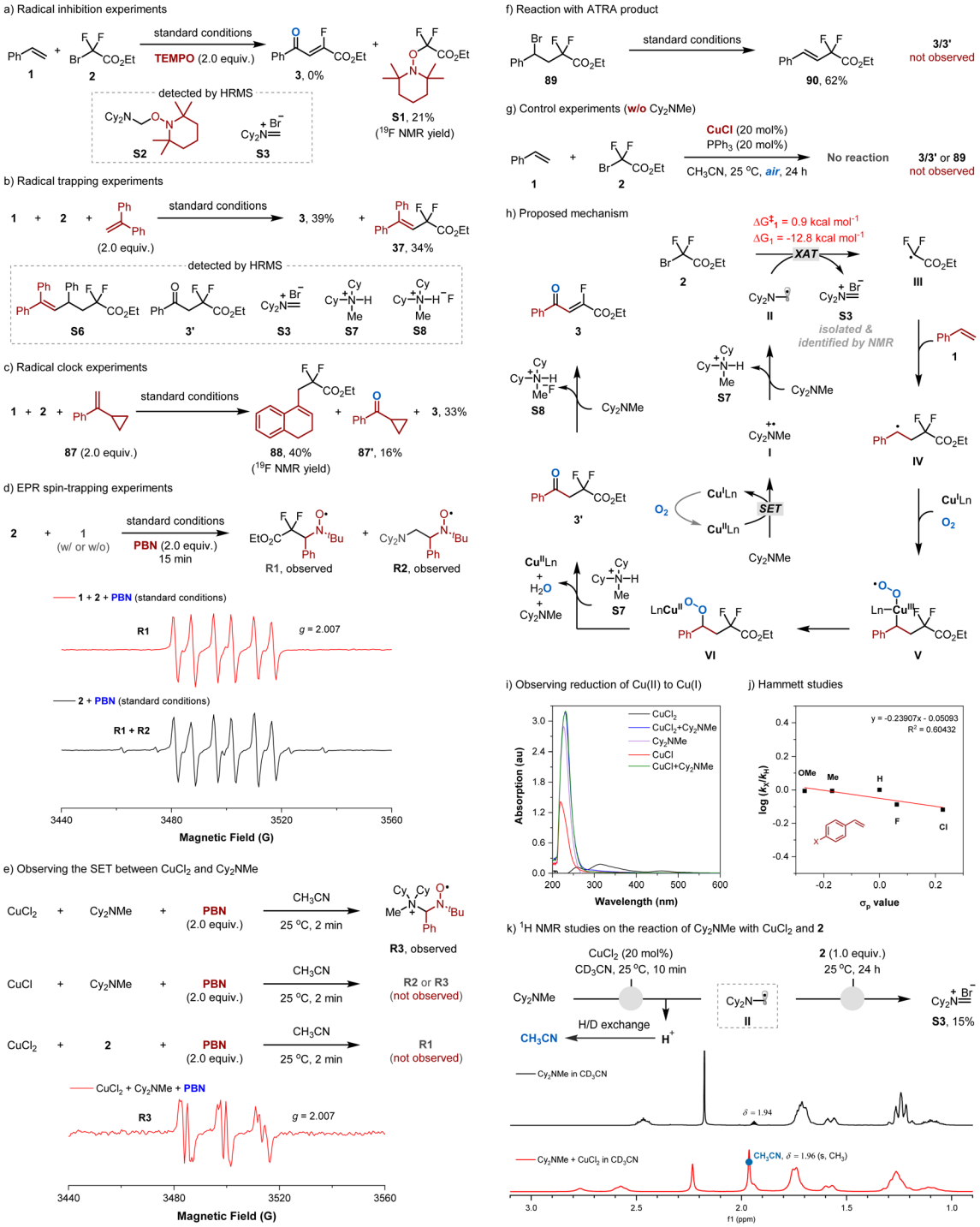

Scheme 5 Mechanistic studies.

observed, corresponding to Cu(II) and (Fig. S11).[65] Although PPh_3 is not essential for product formation, its presence enhance the reaction yield. To elucidate its role, we conducted cyclic voltammetry studies (Fig. S35). The oxidation peak of Cy_2NMe was observed at +0.71 V (*vs.* Ag/AgCl) in CH_3CN,[28,66] while $CuCl_2$ exhibited an oxidation peak at +0.61 V (*vs.* Ag/AgCl),[67] indicating that the SET oxidation of Cy_2NMe by $CuCl_2$ is thermodynamically unfavorable. Notably, mixing $CuCl_2$ with PPh_3, resulted in a new peak at + 0.99 V (*vs.* Ag/AgCl), suggesting the formation of a Cu(II)L_n complex as the active oxidant at the onset of the reaction.[68] We further performed ^{31}P NMR analysis of the reaction mixture to probe the fate of PPh_3 at the end of the reaction. As shown in Fig. S36, the spectrum displayed a single resonance at $\delta \approx 27$ ppm, corresponding to triphenylphosphine oxide ($OPPh_3$), with no detectable signal for unreacted PPh_3.[69,70] This indicates complete oxidation of PPh_3

to $OPPh_3$ under the reaction conditions, likely mediated by the copper catalyst and molecular oxygen, consistent with previous reports on copper-catalysed aerobic phosphine oxidation.[71] Accordingly, the complete conversion of PPh_3 to $OPPh_3$ supports a copper-mediated oxidation mechanism. We cannot exclude the possibility that copper–dioxygen species function as one-electron oxidizing agents for the tertiary amine during the process.[34,35,72] Taken together, these results suggest that the amine radical cation is formed *via* single-electron oxidation of Cy_2NMe by Cu(II) species, and the difluoroacetate radical is generated *via* an XAT process from the α-aminoalkyl radical, rather than from a Cu(II) complex. Additionally, the reaction of the ATRA product **89** did not yield the expected difunctionalisation products **3** or **3′** under standard conditions (Scheme 5f), ruling out an ATRA mechanism.[5,21,73] Finally, the reaction of **1** and **2** with a CuCl catalyst, conducted in the absence of Cy_2NMe under standard conditions, was found to be inefficient (Scheme 5g and Fig. S15). Moreover, no EPR signal was observed in the mixture of CuCl, **2**, and PBN, either in the presence or absence of PPh_3 under these conditions (Fig. S12 and S13). In addition, stirring a mixture of CuCl, **2**, and PPh_3 in CH_3CN at 25 °C for 24 h under air-equilibrated conditions resulted in quantitative recovery of **2**, indicating no detectable consumption (Fig. S14). Taken together, these findings suggest that Cu(I) is unlikely to engage in direct oxidative addition[74,75] or SET[5,21,73] with **2** to generate the ethyl difluoroacetate radical under the tested conditions.

Based on our experimental observations and previous insights, a catalytic cycle that accounts for this transformation is outlined in Scheme 5h. The cycle initiates with a Cu(II)-mediated SET oxidation of Cy_2NMe,[33,36,72,76] leading to the formation of a Cu(I) complex and the amine radical cation **I**. Cu(I) complexes are reoxidized by atmospheric O_2, regenerating Cu(II) complexes.[77] Meanwhile, the amine radical cation rapidly undergoes deprotonation in the presence of base to form the α-aminoalkyl radical **II**.[66,78] A subsequent XAT between the α-aminoalkyl radical **II** and ethyl bromodifluoroacetate (**2**) produces the ethyl difluoroacetate radical **III** and the iminium ion **S3**.[18,26,29,79] The ethyl difluoroacetate radical **III** then adds to styrene (**1**), forming a new C-centered radical **IV**,[79,80] which recombines with Cu(I) and O_2 to yield the Cu(III)-peroxyl radical **V**.[81] The Cu(III) species **V** undergoes rapid rearrangement to produce **3′** and regenerate the Cu(II) species.[81,82] Finally, (*Z*)-β-fluoroenone **3** is formed *via* a dehydrofluorination process in the presence of Cy_2NMe.[83]

Additionally, the formation of Cu(I) species was confirmed through UV-vis spectral analysis (Scheme 5i).[19,82,84] The UV-vis spectrum of $CuCl_2$ shows a band at 460 nm, which disappears upon the addition of Cy_2NMe, accompanied by the appearance of a new band at 230 nm. Similarly, CuCl in the presence of Cy_2NMe exhibits a similar spectrum with a λ_{max} at 230 nm. This spectral change supports the idea that Cu(II) preferentially oxidizes Cy_2NMe to form Cu(I) and the amine radical cation **I**, which participates in the reaction, consistent with the EPR spin-trapping results. To further investigate the oxo-alkylation process, a Hammett analysis was performed (Scheme 5j). Competition experiments between phenylacetylene and *para*-substituted styrene derivatives revealed a linear relationship between $\log(k_X/k_H)$ and σ, with a negative slope ($\rho = -0.23$), suggesting that the transition state is stabilized by electron-donating substituents. This finding supports a mechanism involving radical addition to the double bond, followed by the formation of a Cu(III) intermediate.[85,86] Moreover, the reaction of Cy_2NMe with $CuCl_2$ and **2** at 25 °C in CD_3CN was monitored by NMR spectroscopy (Scheme 5k and Fig. S37). As expected, ^1H NMR revealed the liberation of a proton (H/D exchange forming CH_3CN) during the deprotonation of the amine radical cation **I**, along with the generation of iminium ion **S3** during the XAT process. These results further support the involvement of the α-aminoalkyl radical in the XAT process. Moreover, density functional theory (DFT) calculations suggest that the XAT activation of fluoroalkyl reagents by an α-aminoalkyl radical is favorable both kinetically and thermodynamically (Fig. S41). In addition, the iminium ion **S3** could be isolated by filtration and was well-characterized by NMR and HRMS analysis (Fig. S37 and S38), providing additional evidence that the ethyl difluoroacetate radical is generated *via* XAT mediated by the α-aminoalkyl radical, rather than by Cu(II) species.

Conclusions

In summary, we have developed a copper-catalysed, α-aminoalkyl radical-mediated XAT protocol for the difunctionalisation of diverse styrenes with alkyl halides under air-equilibrated conditions. This method enables divergent access to β-(fluoro) alkylated ketones with broad substrate scope, excellent functional group tolerance, and suitability for late-stage modification of complex bioactive molecules. The reaction is scalable and operationally simple, demonstrating its practical utility. Compared to recently developed catalytic methods that utilize ligated boryl radicals under photoredox conditions,[17,87,88] this straightforward approach oxidizing readily available amines with inexpensive Cu(II) facilitates the formation of α-aminoalkyl radicals, offering an alternative strategy for directly activating fluoroalkyl- and alkyl halides without requiring peroxides[19,25,89] or photoredox conditions.[21] We anticipate this modular approach will be valuable to both academic and industrial chemists. Ongoing efforts in our laboratory are focused on further investigating and expanding the scope of these transformations.

Author contributions

H. F., X. X. and Z. H. conceived and supervised the project. Q. T. and Y. Z. performed the synthetic experiments and analyzed the data. X. L. participated in theoretical calculations. X. L., H. F. and Z. H. participated in the discussions. H. F. and Z. H. co-wrote the manuscript. H. F., X. X. and Z. H. revised and polished the manuscript. All author discussed the results and commented on the manuscript.

Conflicts of interest

There are no conflicts to declare.

Data availability

Supplementary information: The data supporting this article have been included as part of the SI. See DOI: https://doi.org/10.1039/d5sc03774c.

Acknowledgements

The authors are grateful for the financial support from the National Natural Science Foundation of China (22101159, 22171168), National Science Foundation of Shandong Province (ZR2022YQ11), and Hongshen Young Scholars Program from Chongqing University (0247005203005). Special thanks to Prof. Hanmin Huang (USTC), Prof. Zhi-Xiang Yu (PKU) and Prof. Deshuang Tu (NJU) for their helpful discussions and suggestions. The authors are grateful to the supports from Shandong Key Laboratory of next-generation high-performance OLED display material.

Notes and references

1 X. Wu and C. Zhu, *Acc. Chem. Res.*, 2020, **53**, 1620–1636.
2 M. Beller, J. Seayad, A. Tillack and H. Jiao, *Angew. Chem., Int. Ed.*, 2004, **43**, 3368–3398.
3 Z.-L. Li, G.-C. Fang, Q.-S. Gu and X.-Y. Liu, *Chem. Soc. Rev.*, 2020, **49**, 32–48.
4 S. Crespi and M. Fagnoni, *Chem. Rev.*, 2020, **120**, 9790–9833.
5 C. Rao, T. Zhang, H. Liu and H. Huang, *Nat. Catal.*, 2023, **6**, 847–857.
6 F.-F. Tong, Y.-C. Luo, H.-Y. Zhao, X.-P. Fu and X. Zhang, *Angew. Chem., Int. Ed.*, 2025, **64**, e202417858.
7 S. Wang, D. Ren, Z. Liu, D. Yang, P. Wang, Y. Gao, X. Qi and A. Lei, *Nat. Synth.*, 2023, **2**, 1202–1210.
8 C. Rao, T. Zhang and H. Huang, *Nat. Commun.*, 2024, **15**, 7924.
9 Z.-P. Bao, Y. Zhang and X.-F. Wu, *Chem. Sci.*, 2022, **13**, 9387–9391.
10 J. Wang, Q. Zhou, L. Zhou and Z. Zhang, *ACS Catal.*, 2024, **14**, 18499–18506.
11 D. Lu, Y. Li, P. Wang, Z. Wang, D. Yang and Y. Gong, *ACS Catal.*, 2022, **12**, 3269–3278.
12 J. Yu, N.-Y. Yang, J.-T. Cheng, T.-Y. Zhan, C. Luan, L. Ye, Q.-S. Gu, Z.-L. Li, G.-Q. Chen and X.-Y. Liu, *Org. Lett.*, 2021, **23**, 1945–1949.
13 A. Reichle, M. Koch, H. Sterzel, L.-J. Großkopf, J. Floss, J. Rehbein and O. Reiser, *Angew. Chem., Int. Ed.*, 2023, **62**, e202219086.
14 X. Hou, H. Liu and H. Huang, *Nat. Commun.*, 2024, **15**, 1480.
15 R. K. Dhungana, A. Granados, V. Ciccone, R. T. Martin, J. Majhi, M. Sharique, O. Gutierrez and G. A. Molander, *ACS Catal.*, 2022, **12**, 15750–15757.
16 R. Giri, E. Zhilin and D. Katayev, *Chem. Sci.*, 2024, **15**, 10659–10667.
17 C.-Z. Fang, B.-B. Zhang, Y.-L. Tu, Q. Liu, Z.-X. Wang and X.-Y. Chen, *J. Am. Chem. Soc.*, 2024, **146**, 26574–26584.
18 T. Constantin, M. Zanini, A. Regni, N. S. Sheikh, F. Juliá and D. Leonori, *Science*, 2020, **367**, 1021–1026.
19 Z. Zhang, B. Górski and D. Leonori, *J. Am. Chem. Soc.*, 2022, **144**, 1986–1992.
20 X. Sun and K. Zheng, *Nat. Commun.*, 2023, **14**, 6825.
21 T. D. Ho, B. J. Lee, C. Tan, J. A. Utley, N. Q. Ngo and K. L. Hull, *J. Am. Chem. Soc.*, 2023, **145**, 27230–27235.
22 G. Liu, K. Gao, T. Yao, H. Hu and Z. Wang, *Angew. Chem., Int. Ed.*, 2025, **64**, e202500781.
23 D. Wu, S. Wang, H. Zhang, H. Ke, Z. Sun, S. Xie, Y. Gao, J. Yang, B. Wang and X. Lei, *J. Am. Chem. Soc.*, 2025, **147**, 25508–25516.
24 R. K. Neff, Y.-L. Su, S. Liu, M. Rosado, X. Zhang and M. P. Doyle, *J. Am. Chem. Soc.*, 2019, **141**, 16643–16650.
25 B. Górski, A.-L. Barthelemy, J. J. Douglas, F. Juliá and D. Leonori, *Nat. Catal.*, 2021, **4**, 623–630.
26 L. Caiger, H. Zhao, T. Constantin, J. J. Douglas and D. Leonori, *ACS Catal.*, 2023, **13**, 4985–4991.
27 Y.-L. Su, L. Tram, D. Wherritt, H. Arman, W. P. Griffith and M. P. Doyle, *ACS Catal.*, 2020, **10**, 13682–13687.
28 T. Zhang and H. Huang, *Angew. Chem., Int. Ed.*, 2023, **62**, e202310114.
29 W. Suo, J.-Q. Qi, J. Liu, S. Sun, L. Jiao and X. Guo, *J. Am. Chem. Soc.*, 2024, **146**, 25860–25869.
30 H. Zhao, A. J. McMillan, T. Constantin, R. C. Mykura, F. Juliá and D. Leonori, *J. Am. Chem. Soc.*, 2021, **143**, 14806–14813.
31 Z.-Y. Xu, Y.-Y. Jiang, W. Su, H.-Z. Yu and Y. Fu, *Chem.–Eur. J.*, 2016, **22**, 14611–14617.
32 D. Kurandina, M. Parasram and V. Gevorgyan, *Angew. Chem., Int. Ed.*, 2017, **56**, 14212–14216.
33 M. L. Deb, S. S. Dey, I. Bento, M. T. Barros and C. D. Maycock, *Angew. Chem., Int. Ed.*, 2013, **52**, 9791–9795.
34 Y. Li, R. Wang, T. Wang, X.-F. Cheng, X. Zhou, F. Fei and X.-S. Wang, *Angew. Chem., Int. Ed.*, 2017, **56**, 15436–15440.
35 S. Nakai, T. Yatabe, K. Suzuki, Y. Sasano, Y. Iwabuchi, J.-Y. Hasegawa, N. Mizuno and K. Yamaguchi, *Angew. Chem., Int. Ed.*, 2019, **58**, 16651–16659.
36 W. Li, W. Liu, D. K. Leonard, J. Rabeah, K. Junge, A. Brückner and M. Beller, *Angew. Chem., Int. Ed.*, 2019, **58**, 10693–10697.
37 V. O. Nyagilo, S. C. Mallojjala and J. S. Hirschi, *ACS Catal.*, 2024, **14**, 4683–4689.
38 F. Pünner, Y. Sohtome, Y. Lyu, D. Hashizume, M. Akakabe, M. Yoshimura, Y. Yashiroda, M. Yoshida and M. Sodeoka, *Angew. Chem., Int. Ed.*, 2024, **63**, e202405876.
39 J. A. Leitch, T. Rossolini, T. Rogova, J. A. P. Maitland and D. J. Dixon, *ACS Catal.*, 2020, **10**, 2009–2025.
40 K. Sachidanandan, B. Niu and S. Laulhé, *ChemCatChem*, 2023, **15**, e202300860.
41 N. Sanosa, B. Peñín, D. Sampedro and I. Funes-Ardoiz, *Eur. J. Org Chem.*, 2022, **34**, e202200420.
42 L. Zhao, Y. Huang, Z. Wang, E. Zhu, T. Mao, J. Jia, J. Gu, X.-F. Li and C.-Y. He, *Org. Lett.*, 2019, **21**, 6705–6709.
43 V. S. Kostromitin, A. O. Sorokin, V. V. Levin and A. D. Dilman, *Chem. Sci.*, 2023, **14**, 3229–3234.
44 X. Xu and X. Li, *Org. Lett.*, 2009, **11**, 1027–1029.
45 M. Briand, E. Magnier, E. Anselmi and G. Dagousset, *Adv. Synth. Catal.*, 2024, **366**, 3494–3499.
46 P. Cherkupally, A. Slazhnev and P. Beier, *Synlett*, 2011, **3**, 331–334.

47 Z. Zhang, X. Li and D. Shi, *Adv. Synth. Catal.*, 2021, **363**, 3348–3353.
48 S. Arora, P. Katiyar, T. Singh and A. Singh, *Org. Lett.*, 2025, **27**, 3617–3621.
49 S. Morand, P. Jubault, J.-P. Bouillon and S. Couve-Bonnaire, *Chem.–Eur. J.*, 2021, **27**, 17273–17292.
50 Y. Han, L. Zhou, C. Wang, S. Feng, R. Ma and J.-P. Wan, *Chin. Chem. Lett.*, 2024, **35**, 108977.
51 M. Lemmerer, M. Schupp, D. Kaiser and N. Maulide, *Nat. Synth.*, 2022, **1**, 923–935.
52 V. Soulard, G. Villa, D. P. Vollmar and P. Renaud, *J. Am. Chem. Soc.*, 2018, **140**, 155–158.
53 G. Tu, C. Yuan, Y. Li, J. Zhang and Y. Zhao, *Angew. Chem., Int. Ed.*, 2018, **57**, 15597–15601.
54 W.-T. Fan, Y. Li, D. Wang, S.-J. Ji and Y. Zhao, *J. Am. Chem. Soc.*, 2020, **142**, 20524–20530.
55 E. Shirakawa, X. Zhang and T. Hayashi, *Angew. Chem., Int. Ed.*, 2011, **50**, 4671–4674.
56 Z. Feng, Q.-Q. Min, H.-Y. Zhao, J.-W. Gu and X. Zhang, *Angew. Chem., Int. Ed.*, 2015, **54**, 1270–1274.
57 N. Rao, Y.-Z. Li, Y.-C. Luo, Y. Zhang and X. Zhang, *ACS Catal.*, 2023, **13**, 4111–4119.
58 A. L. G. Kanegusuku and J. L. Roizen, *Angew. Chem., Int. Ed.*, 2021, **60**, 21116–21149.
59 W. Li, R. Liu, R. Li, S. Wang, D. Li and J. Yang, *Adv. Synth. Catal.*, 2021, **363**, 5266–5271.
60 H.-Y. Zhao, Z. Feng, Z. Luo and X. Zhang, *Angew. Chem., Int. Ed.*, 2016, **55**, 10401–10405.
61 A. Alberti, M. Benaglia and D. Macciantelli, *Org. Lett.*, 2000, **2**, 1553–1555.
62 G. R. Buettner, *Free Radical Biol. Med.*, 1987, **3**, 259–303.
63 P. Biswas, A. Maity, M. T. Figgins and D. C. Powers, *J. Am. Chem. Soc.*, 2024, **146**, 30796–30801.
64 X. Guo, H. Wang, Z. Hu, Y. Zhao, J. Dong, K. Zhong, Y. Lan and X. Xu, *ACS Catal.*, 2025, **15**, 5307–5317.
65 Y. Abderrazak and O. Reiser, *ACS Catal.*, 2024, **14**, 4847–4855.
66 P.-F. Yuan, Z. Yang, S.-S. Zhang, C.-M. Zhu, X.-L. Yang and Q.-Y. Meng, *Angew. Chem., Int. Ed.*, 2024, **63**, e202313030.
67 L. Xu, J. Xu, J. Zhu, Z. Yao, N. Yu, W. Deng, Y. Wang and B.-L. Lin, *Angew. Chem., Int. Ed.*, 2019, **58**, 6070–6073.
68 F. M. Dennis, A. R. Arenas, M. Shanmugam and B. M. Partridge, *Chem. Eur. J.*, 2024, **30**, e202303636.
69 X. Zhang, H. Liu, X. Hu, G. Tang, J. Zhu and Y. Zhao, *Org. Lett.*, 2011, **13**, 3478–3481.
70 J. Xiao, J. Wang, H. Zhang, J. Zhang and L.-B. Han, *J. Org. Chem.*, 2023, **88**, 3909–3915.
71 H.-J. Zhang, A. W. Schuppe, S.-T. Pan, J.-X. Chen, B.-R. Wang, T. R. Newhouse and L. Yin, *J. Am. Chem. Soc.*, 2018, **140**, 5300–5310.
72 J.-S. Tian and T.-P. Loh, *Angew. Chem., Int. Ed.*, 2010, **49**, 8417–8420.
73 S. Engl and O. Reiser, *Chem. Soc. Rev.*, 2022, **51**, 5287–5299.
74 M.-C. Belhomme, D. Dru, H.-Y. Xiong, D. Cahard, T. Besset, T. Poisson and X. Pannecoucke, *Synthesis*, 2014, **46**, 1859–1870.
75 D. Li, T. Mao, J. Huang and Q. Zhu, *J. Org. Chem.*, 2018, **83**, 10445–10452.
76 T. P. Nicholls, G. E. Constable, J. C. Robertson, M. G. Gardiner and A. C. Bissember, *ACS Catal.*, 2016, **6**, 451–457.
77 B. Zhu, T. Shen, X. Huang, Y. Zhu, S. Song and N. Jiao, *Angew. Chem., Int. Ed.*, 2019, **58**, 11028–11032.
78 Y. Shen and T. Rovis, *J. Am. Chem. Soc.*, 2021, **143**, 16364–16369.
79 W.-J. Yue, C. S. Day, A. J. B. Rucinski and R. Martin, *Org. Lett.*, 2022, **24**, 5109–5114.
80 S. Jana and N. Cramer, *J. Am. Chem. Soc.*, 2024, **146**, 35199–35207.
81 H. Y. Kim and K. Oh, *Org. Biomol. Chem.*, 2021, **19**, 3569–3583.
82 N. Katta, Q.-Q. Zhao, T. Mandal and O. Reiser, *ACS Catal.*, 2022, **12**, 14398–14407.
83 K. Fuchibe, H. Hatta, K. Oh, R. Oki and J. Ichikawa, *Angew. Chem., Int. Ed.*, 2017, **56**, 5890–5893.
84 T. D. Ho, B. J. Lee, T. L. Buchanan, M. E. Heikes, R. M. Steinert, E. G. Milem, S. T. Goralski, Y.-N. Wang, S. Lee, V. M. Lynch, M. J. Rose, K. R. Mitchell-Koch and K. L. Hull, *J. Am. Chem. Soc.*, 2024, **146**, 25176–25189.
85 W. S. Yoon, W. J. Jang, W. Yoon, H. Yun and J. Yun, *Nat. Commun.*, 2022, **13**, 2570.
86 J. Ren, K. Liu, N. Wang, X. Kong, J. Li and K. Li, *ACS Catal.*, 2023, **13**, 11001–11011.
87 Z. Zhang, M. J. Tilby and D. Leonori, *Nat. Synth.*, 2024, **3**, 1221–1230.
88 T. Wan, L. Capaldo, D. Ravelli, W. Vitullo, F. J. de Zwart, B. de Bruin and T. Noël, *J. Am. Chem. Soc.*, 2023, **145**, 991–999.
89 Z. Zhang, L. Poletti and D. Leonori, *J. Am. Chem. Soc.*, 2024, **146**, 22424–22430.